Title: Intrinsic Architecture of Global Signal Topography and Its Modulation by Tasks

Jianfeng Zhang [a,b,*], Zirui Huang [c], Shankar Tumati [d], Georg Northoff [b,d,e,f,*]

[a] College of Biomedical Engineering and Instrument Sciences, Zhejiang University, China

[b] Mental Health Center, Zhejiang University School of Medicine, Hangzhou, Zhejiang Province, China

[c] Department of Anesthesiology and Center for Consciousness Science, University of Michigan, Ann Arbor, 48105, USA

[d] Institute of Mental Health Research, University of Ottawa, Ottawa, ON, K1Z 7K4, Canada

[e] Center for Cognition and Brain Disorders, Hangzhou Normal University, Hangzhou, China

[f] Graduate Institute of Humanities in Medicine, Taipei Medical University, Taipei, Taiwan

* To whom correspondence may be addressed: Jianfeng Zhang, College of Biomedical Engineering and Instrument Sciences, Zhejiang University, Hangzhou, China 310027. E-mail: jianfeng_zhang@zju.edu.cn; or Georg Northoff, Mind, Brain Imaging and Neuroethics, Canada Research Chair, EJLB-Michael Smith Chair for Neuroscience and Mental Health, Royal Ottawa Healthcare Group, University of Ottawa, Institute of Mental Health Research, 1145 Carling Avenue, Room 6467, Ottawa, Canada. E-mail: georg.northoff@theroyal.ca

Abbreviated title: Intrinsic Functional Architecture of Global Signal Topography

Abstract

Recent resting-state fMRI studies reveal that the global signal (GS) exhibits a non-uniform spatial distribution across the gray matter. Moreover, such topography shows spatially preferential alteration across various cognitive and clinical states. One fundamental question about GS topography is whether it is an intrinsic architecture. We here test its existence by using a large sample of fMRI dataset (n=837) from the Human Connectome Project. The GS topography in rest and in seven different tasks are measured by correlating the global signal with the local time series, namely GS correlation (GSCORR). We observe that the topographical pattern of GSCORR in all tasks strongly correlates with the one in rest. The external tasks reduce the mean of GSCORR and slightly modulate the topographical distribution in both task-specific and -unspecific ways. Additionally, this task modulation of GS topography could neither be accounted for by the contribution of subcortical areas linked to arousal level, nor be exclusively explained by physiological noise. Finally, we observe that phase coherence, rather than amplitude variation, serves as the neural basis of GS architecture. Together, we here provide evidence for an intrinsic architecture of GS across rest and various task states.

Keywords: human connectome project, resting state, task modulation

Introduction

A large number of resting state functional connectivity MRI studies have been used in revealing the spatiotemporal organization of the human brain. In the absence of behavioral tasks, fluctuations of spontaneous brain activity exhibit a topography resembling the brain networks known to support overt behavior (1, 2). Recent studies further reveal that the spatial organization of resting state networks remains largely preserved across various tasks, suggesting the existence of an intrinsic architecture of functional networks holding across rest and task states (3, 4).

The global signal (GS) is a major confound in investigating the network organization in resting-state fMRI (5, 6). Global signal in fMRI is defined as the spatial average of time varying BOLD signals across the brain, and regressing the global signal or not often leads to inconsistent conclusions (7-9). To better determine how to process the global signal regression, one needs to understand its potential neuronal relevance. Recent findings demonstrate that the global signal in fMRI exhibits a high correlation to electrophysiological measures on the cortical level (10, 11) while its global fluctuation may partly stem from subcortical regions (e.g., basal forebrain) (12, 13). Finally, abnormalities in the level of the global signal have been observed in psychiatric disorders like schizophrenia (14) and bipolar disorder (Zhang et al. 2018). Together, these findings underscore the neuronal relevance of the global signal. That leaves open though whether the global signal also contributes to shaping the brain's intrinsic architecture.

Although the global signal is generated by the shared activity across the gray matter, the degree of a specific brain region's BOLD signal may, in part, also be related to regional differences in the topographical representation of GS. Recent evidences during resting state in both monkeys (13) and humans (12, 15, 16) demonstrate that the GS exhibits a non-uniform topographical

distribution across regions, characterized by higher levels of GS representation in primary sensory regions like auditory and visual cortex, and lower levels of GS representation in higher-order cortical regions like the prefrontal cortex. Interestingly, psychiatric subjects suffering from schizophrenia (15), autism spectrum disorder (17, 18) or bipolar disorder (19) show abnormal regional distribution of resting state GS, which is also related to the behavioral changes seen in these patients. A fundamental question thus arises whether GS topography reflects an intrinsic architecture holding across rest and task states remains uninvestigated, though.

An intrinsic architecture will suggest the characterized GS is represented in different degrees in different regions thus showing a specific GS topography that, in addition, should hold across different states, e.g., rest and task including different kinds of tasks. In contrast, the absence of intrinsic GS architecture should go along with different GS topographies in rest and task as well as with task-specific GS topographical representation.

The overarching aim of this study is to investigate whether GS topography exhibits an intrinsic architecture. For that purpose, we utilize a large sample fMRI data set from the Human Connectome Project (HCP) that included two days' resting states and seven different tasks. We first test the robustness of GS topography during different days and states (rest and task). Analogous to the justification of intrinsic architecture of functional networks (3), we assume that an intrinsic architecture of GS topography can be indexed by (i) stability over time, (ii) similarity between rest and task states, and (iii) similarity across various task states entailing mainly task-unspecific changes, e.g. different tasks sharing a similar GS topographical pattern. Secondly, we investigate the modulation of GS topography during different tasks. This served the purpose to demonstrate whether and how external tasks modulate GS topography in either a task-specific or task-unspecific manner. Thirdly, because a task may modulate both the phase and amplitude of

ongoing activity (20, 21), we probe the mechanism underlying rest-task modulation of GS architecture, i.e., amplitude variation or phase coherence. Fourthly, we test whether rest-task modulation of GS on the cortical level stems from contributions of subcortical regions (12) , or consists only of non-neuronal physiological noise (8, 22) to GS architecture.

Results

Existence of an intrinsic GS architecture

To investigate whether the GS topography exhibits an intrinsic GS architecture, we calculated the Pearson correlation (i.e., global signal correlation (GSCORR)) with fisher's z transformation between GS and time course in each grayordinate (i.e., gray matter in cortical and subcortical regions). We quantified the GSCORR topography at a group level by averaging the maps of GSCORR across 837 subjects for rest at two days and seven tasks, respectively. Consistent with previous findings (12, 15), a typical GS topography during rest was observed, with higher GSCORR in sensory regions (visual, auditory and somatosensory regions) and lower in association regions (prefrontal and parietal cortices) (Fig. 1).

We then tested the spatial similarity between rest and tasks to check whether GS has a stable architecture. Firstly, we observed an almost identical GS topography during resting state on two days (r = 0.99), suggesting the reliability of GS topography across time. We next averaged the two resting state GS topographies and tested the similarity in topography between rest and the seven tasks. High correlations were observed between rest and tasks (on average: r = 0.91). Even for the relational task, which was least similar task, the correlation was 0.86. Finally, we checked the correlation between the different tasks, which as expected, was also highly correlated (r = 0.95 on average). Together, the high degrees of spatial similarity between the various states (rest-rest, rest-task, task-task) suggested the existence of an intrinsic GS architecture, as its topographical organisation remained largely unchanged across time, and states.

The stability of GS topography was further observed at an individual level by spatial similarity across subjects. The GSCORR topographies of two days' resting state, and seven tasks were first

averaged within each subject. Similar to the group level result (but at a lower value), the spatial correlation of GSCORR in resting state across subjects was 0.60 on average; the spatial correlation of GSCORR in tasks across subjects was 0.63; and the spatial correlation of GSCORR between rest and tasks across subjects was slightly lower (r = 0.58 on average). The high spatial correlation across subject strongly supports the existence of GS intrinsic architecture.

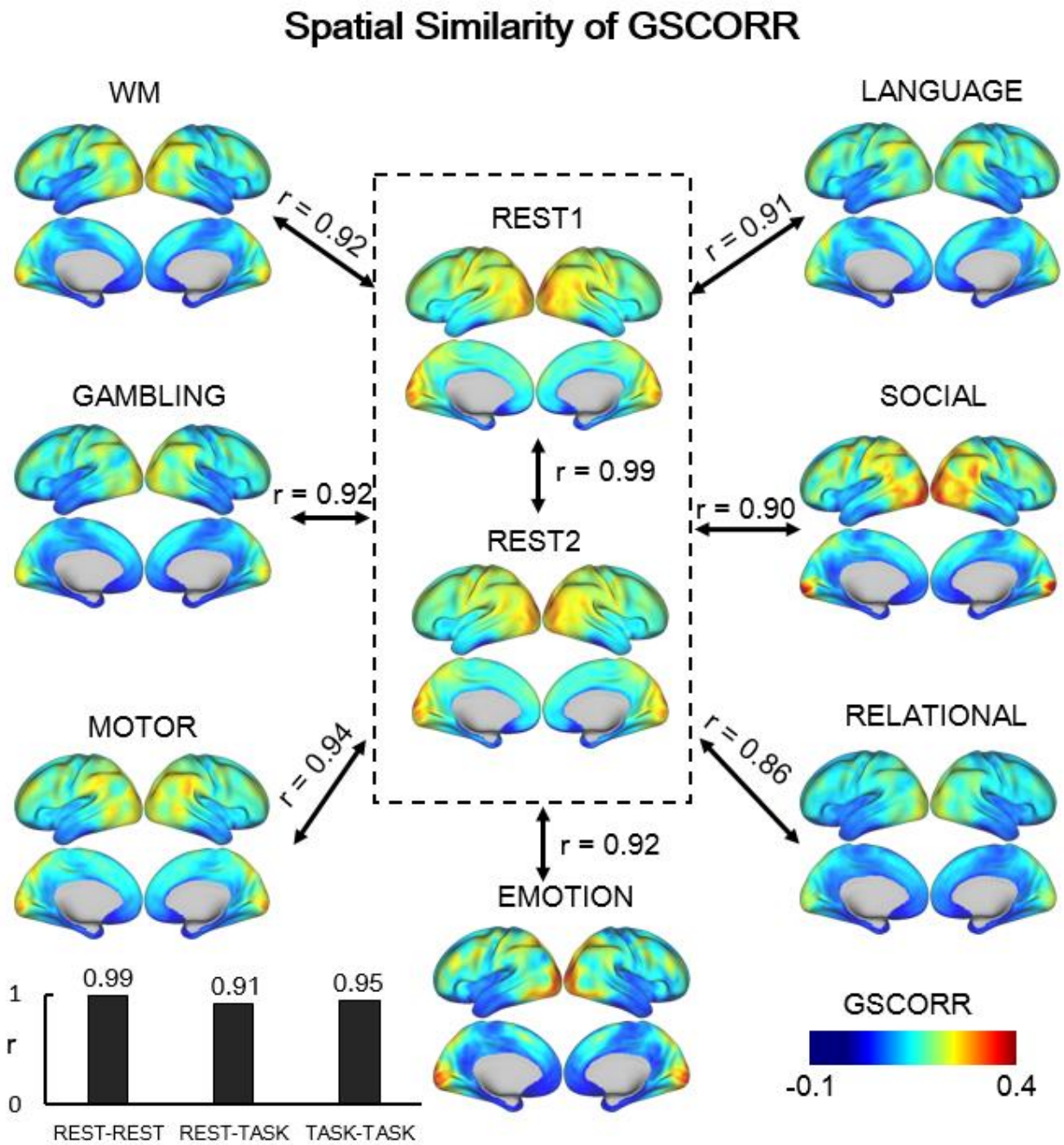

Fig. 1. **Intrinsic architecture of global signal**. The GSCORR is measured as the Pearson's correlation between global signal and time course in each grayordinate with fisher's z transformation. The spatial similarity is measured by Pearson's correlation across grayordinates. Very high similarities are observed between rest in day1 (REST1) and day2 (REST2) (r = 0.99),

between rest and tasks (r = 0.91 in average), and between different tasks (r = 0.95 in average), supporting the existence of an intrinsic GS topography.

Task modulation of intrinsic GS architecture

The intrinsic GS architecture may capture brain's global functional organization, or the spatial pattern of functional irrelevant physiological noise. To clarify the functional relevance of GS architecture, we investigated how the tasks modulate GS topography.

We first investigated the whole-brain averaged GSCORR across time (REST1 and REST2), and state (rest and seven tasks). The comparison of GSCORR within the two rests showed no significant difference despite the large sample size (n=837), while the comparisons of GSCORR between rest and tasks showed a consistent reduction of GSCORR in all tasks (in all contrasts between rest and tasks, $t > 12$, Cohen's $d>0.4$, $p<3.8*10^{-32}$, Bonferroni corrected for eight comparisons (i.e., REST1 vs. REST2, and seven pairs of comparisons between rest and tasks)) (Fig. 2A).

The reduction of whole-brain GSCORR can occur uniformly across all regions in the brain, or, alternatively, can be manifested in a non-uniform way across different regions. By performing grayordinate-based comparison between rest and tasks, we observed non-uniform regional distribution of task modulation of GSCORR. As the sample size was large and therefore easily reached significance, we used the threshold at |Cohen's d| > 0.2 for further analyses (the threshold for reaching small effect size, corresponding to |t-values| > 5.78). A large number of regions showed GSCORR reduction when switching to task state, while only some regions exhibited task-related increase or remained unchanged (Fig. 2B).

We further tested whether the task modulation of GSCORR (i.e., reduced, increased, or unchanged), was task-unspecific or task-specific. For this purpose, we generated the overlapped maps, and calculated the number of task modulations (i.e., reduced, unchanged, or increase) across the seven tasks for each grayordinate (Fig. 2C top panel), and the percentages of grayordinates for the number of each modulation (Fig. 2C bottom panel). For the regions showing GSCORR reduction, 54.2% regions showed reduction in at least 4 tasks (4-7 tasks), while only 18.6% regions showed GSCORR reduction in 1-3 tasks. For those regions that remained unchanged, 41.3% exhibited similar GSCORR values across at least 4 tasks (4-7 tasks), while 33% of these regions remained unchanged in 1-3 tasks. Finally, we refrained from making this calculation in the regions that showed GSCORR increase as their number was rather small and inconsistent across the various tasks (Fig. 2C bottom panel). Together these findings suggest that GSCORR modulation in both type of regions, i.e., reduced and unchanged, was rather task-unspecific as it mostly occurs across the different tasks.

We lastly examined the regional specificity of GSCORR in task modulation. GSCORR reductions were observed mainly in auditory and somatosensory regions as well as in the regions belonging to the DMN. In contrast, the unchanged (plus a small set of increased) regions included the primary visual cortex (six of the seven tasks included visual components/stimuli), and the regions belonging to frontoparietal executive control network and ventral attention network (most of the tasks involved some executive and/or attentional function) (Fig. 2C top panel).

Taken together, we suggested that, while essentially being preserved during task, the intrinsic GS architecture was nevertheless modulated during tasks in mostly task-unspecific ways. Such modulation was mainly manifested in GSCORR reduction in a large set of regions while only some regions exhibited task-related GSCORR increase (and others remained unchanged).

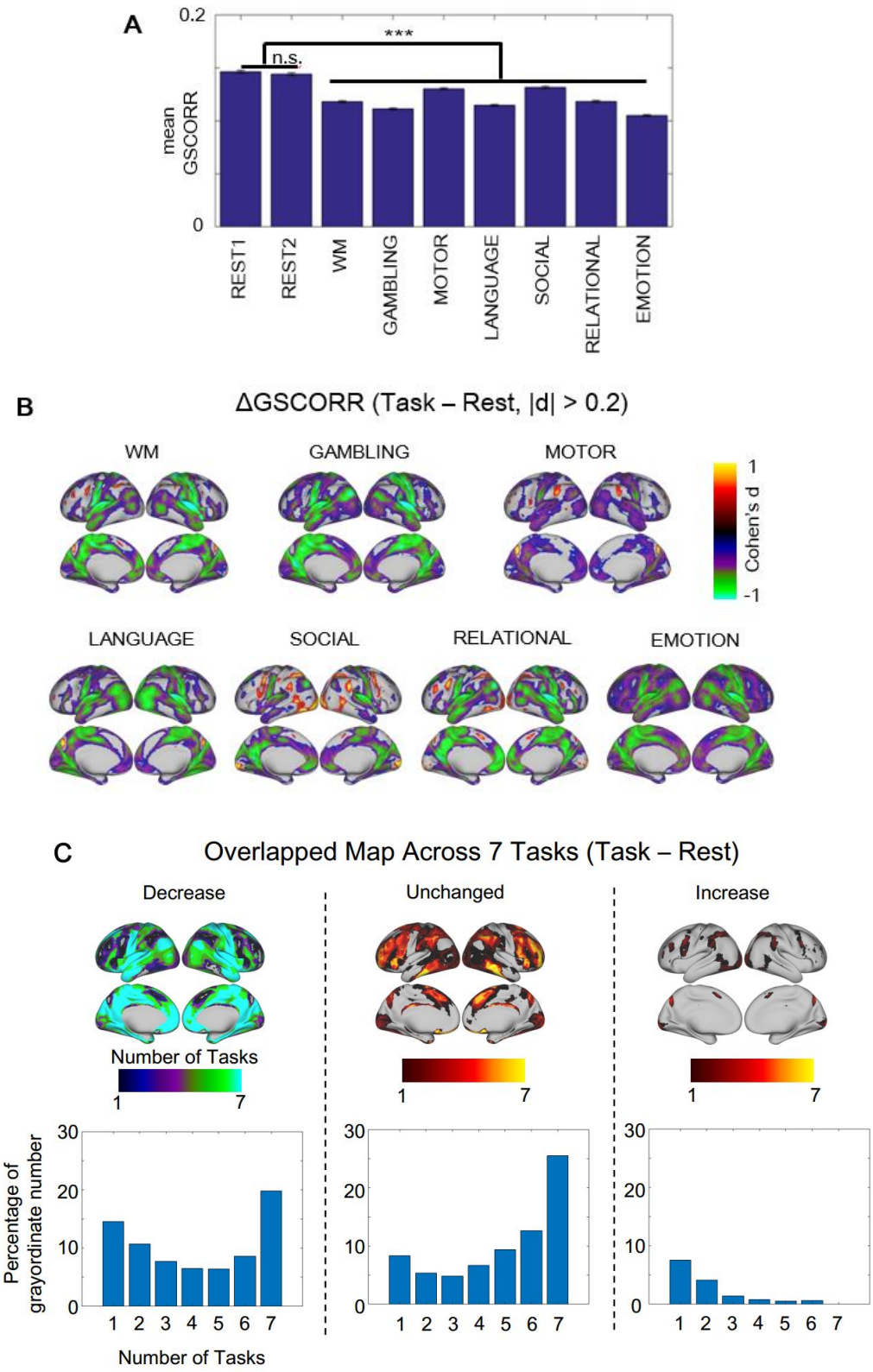
A
0.2
0
mean GSCORR
***
n.s.
REST1
REST2
WM
GAMBLING
MOTOR
LANGUAGE
SOCIAL
RELATIONAL
EMOTION
B
ΔGSCORR (Task – Rest, |d| > 0.2)
WM
GAMBLING
MOTOR
LANGUAGE
SOCIAL
RELATIONAL
EMOTION
1
Cohen's d
-1
C
Overlapped Map Across 7 Tasks (Task – Rest)
Decrease
Unchanged
Increase
Number of Tasks
1
7
Percentage of grayordinate number
30
20
10
0
1 2 3 4 5 6 7
Number of Tasks

Fig. 2. **Task modulation of global signal architecture.** ***A***. whole brain GSCORR in day1 (REST1) and day2 (REST2) rest and seven tasks. ***B***. grayordinate-based group comparison for global signal topography. The maps are thresholded by Cohen's d > |±0.2|. ***C.*** top panel: the overlapped map across 7 tasks illustrate the counted number of each grayordinate showing decrease (left), unchanged (middle), and increase (right) in task when comparing to rest at the level of Cohen's d > |±0.2|. Bottom panel illustrates the percentage of grayordinates for each counted number in overlapped maps.

Phase coherence vs. amplitude variability for rest-task modulation of GSCORR

Previous studies demonstrated that the task-related activity is modulated by both amplitude (20, 23) and phase (21) of the ongoing activity. We therefore tested whether rest-task modulation of GS topography was related to amplitude variation (neural variability) or phase coherence. First, we calculated phase coherence using the Kuramoto index (24, 25) between global signal and each grayordinate (Global signal Kuramoto/GSK). The task modulations between task and rest were calculated by Cohen's d, similar to GSCORR grayordinate-based analysis (see above). Since GSCORR may also be mediated by other mechanisms like amplitude variation (19), we also calculated neural variability, measured by standard deviation (SD) (23, 26-28). All the maps were thresholded at |Cohen's d|>0.2.

To check for similarity or difference in regional distribution, we correlated the spatial topographic maps of GSCORR with those of phase coherence (GSK) and neural variability (SD), respectively. The spatial topographical maps for phase coherence (GSK) showed very high spatial similarity with GSCORR (r-value ranging from 0.79 to 0.96) (Fig. 3) (but differing in their threshold of

significance). In contrast, the spatial maps for SD were clearly different from those of GSCORR with r-values ranging from 0.22 to 0.49 (Fig. 3). Moreover, comparison of the two maps with each other, i.e., phase coherence and neural variability, revealed significant difference (for each pair, $p < 0.001$, Bonferroni corrected). Finally, even the lowest r value in correlation between GSCORR and GSK (0.79) was still significantly higher than the highest one between GSCORR and SD (0.49) (see Figure 3). Together, our findings suggested that task modulation of GSCORR topography are mediated by phase coherence rather than neural variability.

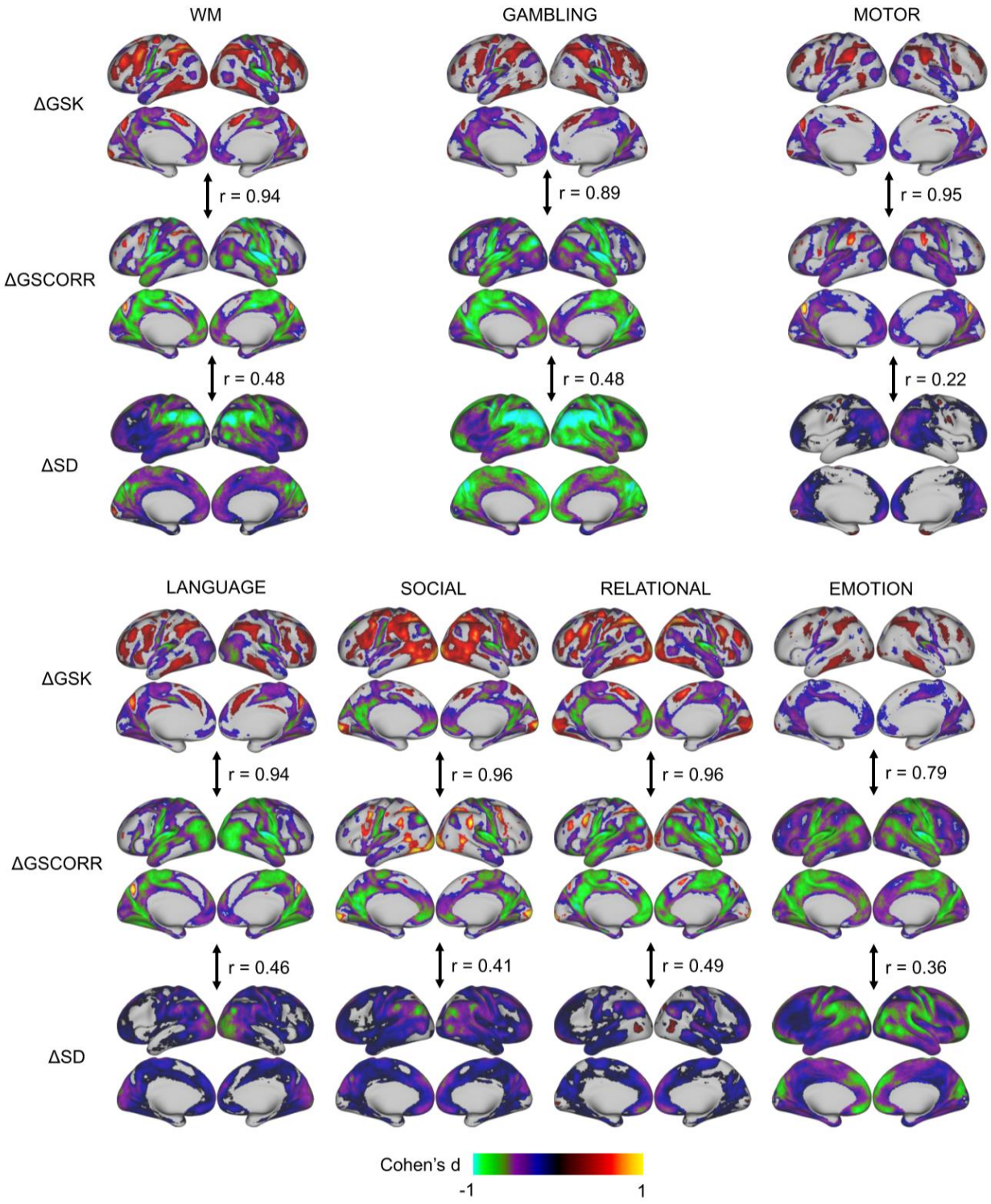

Fig. 3. **Phase vs. amplitude driven task modulation of global signal topography.** Spatial similarity of the task modulated topography (task minus rest) between phase coherence index

(measured here as global signal kuramoto index (GSK) between GS and time course in each grayordinate), GSCORR, and standard deviation (SD). The maps are thresholded by Cohen's d > |±0.2|, but the spatial similarity is measured based on all grayordinates.

Non-cortical GS components to rest-task modulation – Contributions from basal forebrain

A recent study reported that the neural origin of the global signal lies in the basal forebrain which suggests that, at least in part, the global signal may reflect the level of arousal (12, 13). We therefore investigated whether the task modulation of global signal topography is driven by this subcortical region.

We replicated the previous findings in both rests and all tasks, thresholded at |Cohen's d| > 0.2 (Fig. 4, top panel), by showing a negative correlation between basal forebrain and global signal (12, 13). Extending these results, we demonstrated that GS in basal forebrain was not modulated during different tasks when compared to rest as manifested in the absence of any significant rest-task difference (see Fig. 4 bottom panel). This suggested that the task modulation of GS on the cortical level, as described above, was not driven by the basal forebrain's contribution to the global signal.

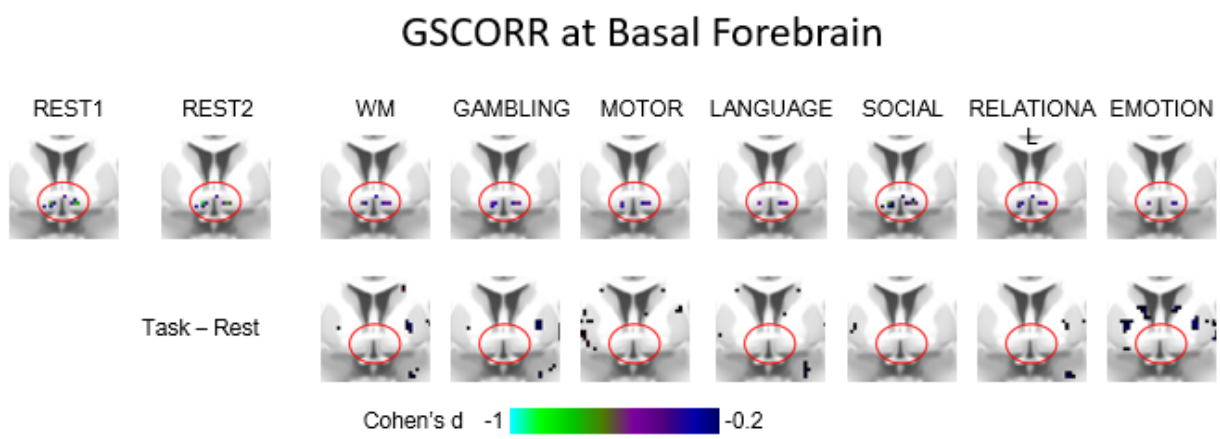

Fig. 4. GSCORR at Basal Forebrain in rest and tasks. The maps are thresholded by Cohen's d > |±0.2|. Top panel, group GSCORR comparison with baseline (H0: r = 0). Bottom panel, group comparison which shows no significant difference between rest and task as reflected in the absence of any voxel in the basal forebrain.

Non-cortical GS components to rest-task modulation – Contributions from physiological noise

Finally, as the global signal is affected by noise (8), we checked whether the task modulation of global signal topography was driven by the difference in noise (i.e., head motion, respiration, cardiac, and signal from the ventricle and white matter). We calculated the GSCORR without any noise regression (see methods for details). If task modulation of GSCORR was driven by irrelevant noise, its spatial pattern, as calculated without noise, should show low degrees of spatial similarity to the one of global signal topography with noise regression. Our results showed high correlation, and thus very similar GSCORR spatial pattern before and after nuisance noise regression (r > 0.95 in all cases) (Fig. 5). More importantly, we observed that inclusion of noise regression increased the effect size of GSCORR task modulation in all seven tasks (increased percentage in Cohen's d ranging from 31% to 69%).

Together, these results suggested that global signal topography during rest-task modulation cannot be explained by non-neuronal components in global signal. Instead, regressing out non-neuronal components increased the signal-to-noise ratio, and strengthened the presumed neuronal component of GSCORR in the measured signal.

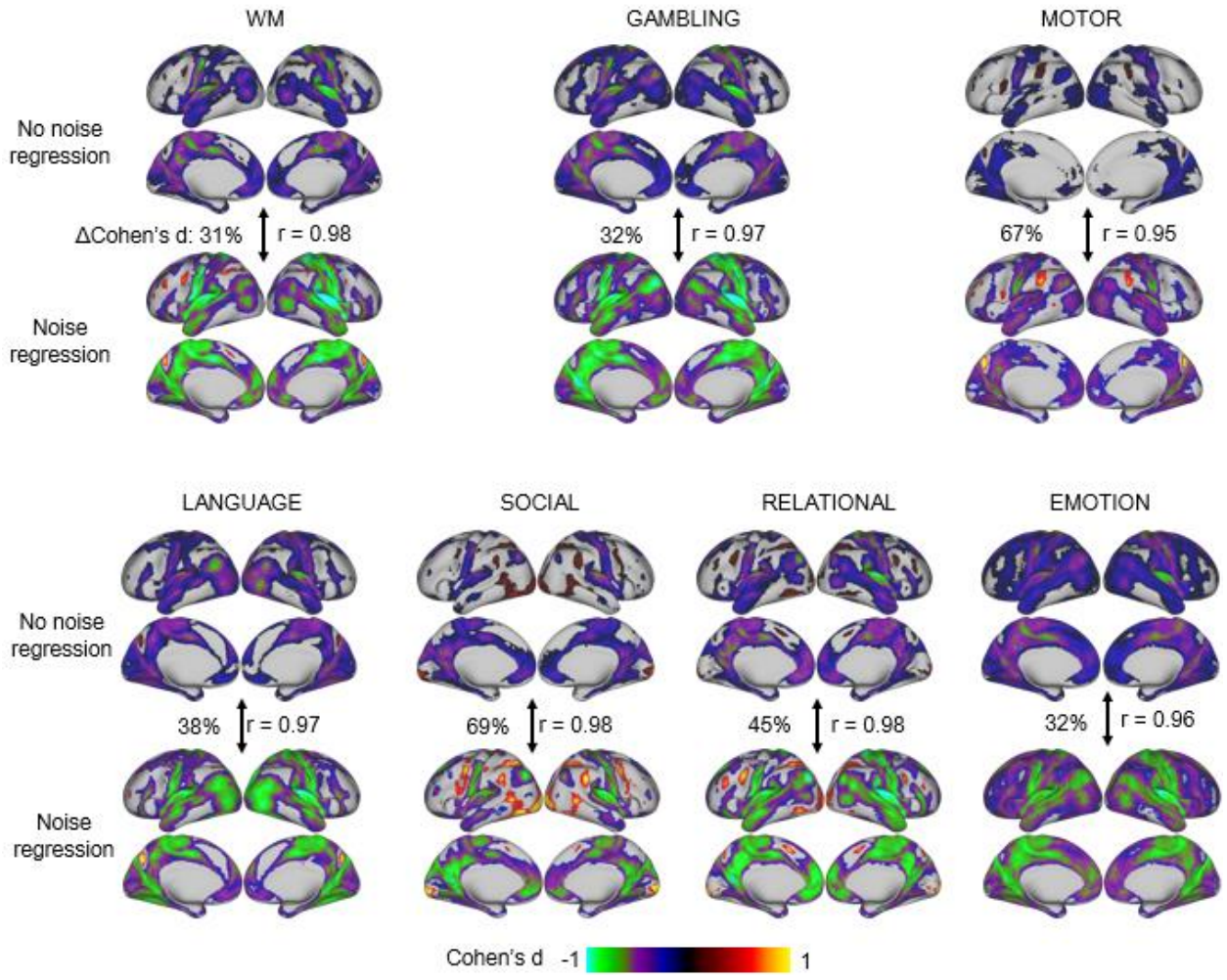

Fig. 5. Physiological noise influence on task modulated GSCORR topography. The maps are thresholded at Cohen's | d | > 0.2. The spatial similarity of task modulation is measured based on the Cohen's d GSCORR topography. The percentage of enhanced effect size after noise regression are calculated as the difference of whole brain Cohen's d with normalization (by dividing Cohen's d before noise regression).

Discussion

Main findings

This study investigated the existence of intrinsic functional architecture in the brain's global activity. We demonstrated the GS topography exhibited a stable spatial pattern across rest and task, supporting the term as intrinsic architecture. Moreover, such GS architecture is modulated during different tasks by showing task-unspecific decreases in GS levels in most regions while GS increases could only be observed in a few task-specific regions, suggesting this topography is functional relevant. The underlying mechanism of rest-task modulation in GS architecture is phase coherence rather than amplitude variation. Moreover, we rule out other potential sources of GS architecture on the cortical level including contributions from subcortical regions and non-neuronal physiological noise. Together, we here demonstrate the existence of an intrinsic functional architecture of the brain's global activity.

Intrinsic architecture of global signal – Preserved topography during rest and task

Our first main finding shows that the global signal distribution as measured by GSCORR exhibits an extremely high degree of spatial similarity across different states. The spatial pattern of GSCORR levels in different regions highly correlated not only among the two resting states (as expected) but also between rest and task as well as between the different tasks. The topography of GSCORR is thus preserved throughout the different states; this strongly supports the assumption of the brain's global activity (as measured by GSCORR) exhibiting an intrinsic architecture.

The existence of an intrinsic architecture in the brain's activity present during both rest and task

states is in-line with findings of functional connectivity in functional networks. In a series of papers, Cole and colleagues (3, 4, 29, 30) demonstrated a network-based intrinsic architecture, based on inter-regional functional connectivity, that is preserved during both rest and task states. The observation of such intrinsic architecture on the network level complements analogous architectures on both anatomical-structural (31) and biochemical (32) levels. We extend the assumption of the brain's intrinsic architecture by demonstrating it on the level of the brain's global activity as distinct from network, anatomical, and biochemical levels. Our results show a consistency of GS topographical pattern across time, subjects, and states, e.g., rest and task. Moreover, the observed global intrinsic architecture shapes and structures different task states in more or less similar ways. Together, these findings support the view of the existence of an intrinsic architecture of GS. Future studies are warranted to investigate how the global level of the brain's intrinsic architecture stands in relation to the topographical pattern on anatomical, biochemical, and network levels.

Functional relevance of global signal intrinsic architecture – spatial distribution and task modulation

We demonstrate that the GS exhibits a non-uniform topographical distribution across regions, characterized by higher levels of GSCORR in primary sensory regions like auditory and visual cortex, and lower levels of GSCORR in higher-order cortical regions like the prefrontal cortex. This replicates recent findings during resting state in both monkeys (13) and humans (12, 15, 16). Importantly, GS topography is altered in psychiatric disorders, with abnormal GS levels in symptom related regions (15, 19). Together, these findings in abnormal conditions suggest that GS topography is functionally relevant as for cognition and behavior.

The present findings demonstrate that GS topography is modulated during different tasks in largely task-unspecific ways, e.g., task-unspecific decreases, as well as, in a small number of regions by task-specific GS increases. These findings suggest that GS topography is not only present during rest but also shapes task-related activity in different regions in both task-unspecific and task-specific ways. Hence, task-related activity may be conceived a hybrid of both the impact of the task itself and its modulation by GS topography including task-specific and task-unspecific shaping in different regions.

We observed that the level of GSCORR decreased in various regions across the different tasks, reflecting task-unspecific responses. In contrast, GSCORR increased in only a few regions which were also limited to specific tasks thus being more task-specific. Finally, a third set of regions do not show any GSCORR change at all during task states. Overall our data suggest that GS topography is modulated during tasks predominantly in a task-unspecific (rather than task-specific) way.

Mechanism of global brain activity – phase coherence

The underlying mechanisms mediating the global activity during rest-task modulation remains unclear so far. Previous authors suggest either neuronal variability (14) or phase coherence (21, 33-36) to underlie the global signal. We therefore tested whether GS topography during rest-task modulation is more similar to phase- or, alternatively, amplitude-based signal distributions of global neural activity. Our data show high correlation of GS rest-task modulation maps with the topographical maps of phase-based analysis of the same data. In contrast, no such high correlation is observed with amplitude-based topography. These data let us suggest that GS topography

including its rest-task modulation is strongly driven by phase coherence rather than neural variability (as measured by SD).

Recent studies in both fMRI (21, 34, 35) and ECoG (36) strongly suggest that functional connectivity is phase-based and thus reflects the fluctuations in the coherence between different voxels/regions. Combined with our findings, we extend these results to the global signal. We assume that GS reflects the phase-based coherence between all voxels/regions on a global level. Task-unspecific decreases in GS may then be related to phase-based decoupling or desynchronization of local or regional activity from the overall global activity. Thus, the global activity may ultimately operate through the degree of phase coherence between global and local (or regional) activity. On a more processing and informational level, such phase-based mechanisms underlying global activity may account for the balance between (global) integration and (local) differentiation (37, 38).

Subcortical and physiological substrate underlying intrinsic global signal architecture

Global signal is subject to controversy as its exact neuronal basis is not fully clear yet (8, 22). Recent studies demonstrate that the basal forebrain plays a special role in determining global resting-state fluctuations in both human (12) and macaque (13). This region is functionally involved with arousal or vigilance regulation (39-42). We here replicate the contribution of basal forebrain to global signal in both rest and all tasks (Fig. 4 top panel). However, the rest-task interaction is not explained by the contribution of basal forebrain to global signal (Fig. 4 bottom panel). This suggests that the global signal may stem or originate in a variety of different neural substrates, including both subcortical projection and cortical synchronization. While the spatial

organization of global signal, i.e., its intrinsic architecture, may relate mainly to its cortical component, e.g., cortical synchronization. However, further investigations by isolating the different components in global signal are warranted to illustrate the topography of each component.

Global signal also partly includes the widespread non-neuronal noise. For this reason, global signal is usually regressed and thus eliminated from the data (8, 22). However, recent evidence relating electrophysiological and fMRI measures suggest that the GS is not merely physiological noise but also contains important neuronal activity (12, 13, 43). Our data provide further support to this view by showing the functional relevance of GS topography, which may root to the neuronal activity containing in GS. We showed highly correlating and thus similar topographical distribution of rest-task GS modulation both with and without physiological noise regression (Fig 5). If the GS topography only reflected spatial pattern of non-neuronal noise, one would have expected the opposite - namely, low or no correlation in GS topography between analyses with and without physiological noise regression. However, further investigations of GS topography using electrophysiology is necessary to corroborate its assumed neuronal basis.

Conclusion

We here demonstrate an intrinsic functional architecture of the brain's global activity as measured by the global signal in fMRI. This is well reflected in the preserved topography of GS during both rest and tasks. Moreover, we show predominant task-unspecific GS decreases or no change in various regions, while only a few regions exhibiting task-specific increases in GS. Our findings provide a novel framework for future studies to characterize global signal and its topography during task states in both healthy and psychiatric subjects.

355

Materials and Methods

Data Collection

We utilized data from the Human Connectome Project (HCP) (44, 45). All subjects from the HCP 1200-subject data release (Mar 01, 2017) having completed fMRI sessions with completed physiological recordings (cardiac and respiratory signals) were included (837 subjects in total). The age of the participants in the project ranges from 22 to 35, and 54% were female. Whole-brain echo-planar imaging acquisitions were acquired with a 32-channel head coil on a modified 3T Siemens Skyra with TR = 720 ms, TE = 33.1 ms, flip angle = 52°, BW = 2,290 Hz/Px, in-plane FOV = 208 × 180 mm, 72 slices, 2.0 mm isotropic voxels, with a multiband acceleration factor of 8 (46).

Task paradigms

Data were collected over 2 days. On each day the data collection included 28 min of rest (eyes open with fixation) fMRI data across two runs, and 30 min of task fMRI. Each of the seven tasks was completed over two consecutive fMRI runs (47). These tasks included seven distinct domains: emotion, reward learning, language, motor, relational reasoning, social cognition and working memory. Briefly, the emotion task involved matching fearful or angry faces to a target face. The reward learning task involved a gambling task with monetary rewards and losses. The language task involved auditory stimuli consisting of narrative stories and math problems, along with questions to be answered regarding the prior auditory stimuli. The motor task involved movement of the hands, tongue and feet. The relational reasoning task involved higher-order cognitive reasoning regarding relations among features of presented shape stimuli. The social cognition task

used short video clips of moving shapes that interacted in some way or moved randomly, with subjects making decisions about whether the shapes had social interactions. The working memory (WM) task consisted of a visual N-back task, in which subjects indicate a match of the current image to either a constant target image or two images previous. The details of tasks can be found elsewhere (47).

fMRI data preprocessing

Preprocessing was carried out using Workbranch (48) and custom code in MATLAB 2017b (MathWorks). Spatial image preprocessing (distortion correction and image alignment) was carried out using the HCP's grayordinate-based spatial minimal preprocessing pipelines (49). These pipelines maximize alignment across image modalities, minimize distortions relative to the subject's anatomical space, and minimize spatial smoothing (blurring) of the data. The data were projected into the 2mm standard CIFTI grayordinates space, which includes cortical gray matter surface vertices and subcortical gray matter voxels. This offers substantial improvements in spatial localization over traditional volume-based analyses, enabling more accurate cross-subject and cross-study registrations and avoiding smoothing that mixes signals across differing tissue types or between nearby cortical folds (45, 49).

The within-run intensity was normalized to a whole-brain mode value of 10000. The linear trend for each run were removed, and the nuisance time series (ventricle, white matter, cardiac, respiratory signals, motions along with their derivatives) were regressed by using linear regression (4, 8). The nuisance time series (ventricle, and white matter signals) were extracted from volume-based minimally processed version. No low-pass temporal filter was applied given the possibility

that frequency specificity might differ between rest and task state (4).

Global signal topography

The global signal was calculated for each subject by averaging the fMRI signals across grayordinate. The GS topography was calculated by Pearson correlation (i.e., Global signal correlation/GSCORR) between the global signal and the time series in each grayordinate (5, 8). The correlation r values were then transformed through fisher's z transformation for statistical analyses (3, 4).

Control analysis

To examine whether the global signal topography differed across states due to the difference of nuisance signal contribution (8), we additionally calculated the GS topography without nuisance signal regression in preprocessing (ventricle, white matter, cardiac, respiratory signals, motions alone with their derivatives). The grayordinate-based correlation for the task-rest difference with and without nuisance signal regression was calculated to check the influence of nuisance signal on rest-task difference (28).

Spatial similarity of global signal topography

We first tested the spatial similarity between the different states on the group-level map. For that purpose, we conducted grayordinate-based Pearson correlation between states (i.e., REST (day1) – REST (day2), REST-TASK, TASK-TASK).

Second, we tested the spatial similarity on the individual-level map. The GSCORR topographies of two days' resting state, and seven tasks were first averaged within each subject, respectively. The spatial similarity was then calculated across individuals to check the spatial stability.

Standard Deviation (SD) and phase coherence with global signal in each grayordinate

The contribution to global signal from each grayordinate can depend on either the level of amplitude or the level of phase coherence. To level of amplitude was measured by the standard deviation (SD) of blood oxygenation level-dependent (BOLD) signal, which describes the temporal variability of brain activity across time within voxel (23, 26, 28).

The level of phase coherence was calculated by global signal Kuramoto index (GSK)(24, 25), which measures the averaged phase synchrony across time between global signal and each grayordinate and has been applied in fMRI recently (21, 50). The phase was calculated through Hilbert transform and the phase synchrony as a function of time was quantified by the Kuramoto index, K(t), defined by:

$$\mathrm{K(t)} = \frac{1}{n}\left|\sum_{n}^{1} e^{i\theta_j(t)}\right|$$

where n = 2, as the calculation was performed between global signal and each grayordinate. The overall phase coherence was then defined as the average of Kuramoto index across time (21).

Statistics

Given that in large samples, the *p*-values tend to be significant for small effects, we mainly report

results with a pre-specified effect size using Cohen's d (51). The threshold for the difference in brain maps was set as | Cohen's d | > 0.2 which corresponds to | t-values | > 5.78 ($p < 0.00001$) in the current sample size. All statistical inferences for global signal topography and spatial similarity were based on two-tailed paired t-tests on the Fisher's z-transformed r-value. Person correlation (r) was used to measure the spatial similarity and the effect size of correlation (spatial similarity) was indicated by the r-value.

Acknowledgment

We thank the Human Connectome Project for excellent open-access data. This work is supported by the grant from the Ministry of Science and Technology of China, National Key R&D Program of China (2016YFC1306700), the European Union's Horizon 2020 Framework Programme for Research and Innovation under the Specific Grant Agreement No. 785907 (Human Brain Project SGA2), the EJLB-Michael Smith Foundation, the Canada Institute of Health Research (CIHR), and the Start-up Research Grant in Hangzhou Normal University (G.N.). We declare no conflict of interest.

Reference

1. Biswal B, Zerrin Yetkin F, Haughton VM, Hyde JS. Functional connectivity in the motor cortex of resting human brain using echo-planar MRI. Magnetic resonance in medicine. 1995;34(4):537-41.
2. Fox MD, Raichle ME. Spontaneous fluctuations in brain activity observed with functional magnetic resonance imaging. Nature reviews neuroscience. 2007;8(9):700.
3. Cole MW, Bassett DS, Power JD, Braver TS, Petersen SE. Intrinsic and task-evoked network architectures of the human brain. Neuron. 2014;83(1):238-51.
4. Cole MW, Ito T, Bassett DS, Schultz DH. Activity flow over resting-state networks shapes cognitive task activations. Nat Neurosci. 2016;19(12):1718-26.
5. Fox MD, Zhang D, Snyder AZ, Raichle ME. The global signal and observed anticorrelated resting state brain networks. J Neurophysiol. 2009;101(6):3270-83.
6. Murphy K, Birn RM, Handwerker DA, Jones TB, Bandettini PA. The impact of global signal regression on resting state correlations: are anti-correlated networks introduced? Neuroimage. 2009;44(3):893-905.
7. Power JD, Barnes KA, Snyder AZ, Schlaggar BL, Petersen SE. Spurious but systematic correlations in functional connectivity MRI networks arise from subject motion. Neuroimage. 2012;59(3):2142-54.
8. Power JD, Plitt M, Laumann TO, Martin A. Sources and implications of whole-brain fMRI signals in humans. Neuroimage. 2017;146:609-25.
9. Saad ZS, Gotts SJ, Murphy K, Chen G, Jo HJ, Martin A, et al. Trouble at rest: how correlation patterns and group differences become distorted after global signal regression. Brain connectivity. 2012;2(1):25-32.
10. Schölvinck ML, Maier A, Frank QY, Duyn JH, Leopold DA. Neural basis of global resting-state fMRI activity. Proceedings of the National Academy of Sciences. 2010;107(22):10238-43.
11. Lv Y, Margulies DS, Cameron Craddock R, Long X, Winter B, Gierhake D, et al. Identifying the perfusion deficit in acute stroke with resting-state functional magnetic resonance imaging. Annals of neurology. 2013;73(1):136-40.

12. Liu X, de Zwart JA, Scholvinck ML, Chang C, Ye FQ, Leopold DA, et al. Subcortical evidence for a contribution of arousal to fMRI studies of brain activity. Nat Commun. 2018;9(1):395.

13. Turchi J, Chang C, Ye FQ, Russ BE, Yu DK, Cortes CR, et al. The Basal Forebrain Regulates Global Resting-State fMRI Fluctuations. Neuron. 2018;97(4):940-52 e4.

14. Yang GJ, Murray JD, Repovs G, Cole MW, Savic A, Glasser MF, et al. Altered global brain signal in schizophrenia. Proc Natl Acad Sci U S A. 2014;111(20):7438-43.

15. Yang GJ, Murray JD, Glasser M, Pearlson GD, Krystal JH, Schleifer C, et al. Altered Global Signal Topography in Schizophrenia. Cereb Cortex. 2017;27(11):5156-69.

16. Wen H, Liu Z. Broadband Electrophysiological Dynamics Contribute to Global Resting-State fMRI Signal. J Neurosci. 2016;36(22):6030-40.

17. Gotts SJ, Saad ZS, Jo HJ, Wallace GL, Cox RW, Martin A. The perils of global signal regression for group comparisons: a case study of Autism Spectrum Disorders. Front Hum Neurosci. 2013;7:356.

18. Gotts SJ, Simmons WK, Milbury LA, Wallace GL, Cox RW, Martin A. Fractionation of social brain circuits in autism spectrum disorders. Brain. 2012;135(9):2711-25.

19. Zhang J, Magioncalda P, Huang Z, Tan Z, Hu X, Hu Z, et al. Altered Global Signal Topography and Its Different Regional Localization in Motor Cortex and Hippocampus in Mania and Depression. Schizophr Bull. 2018.

20. He BJ. Spontaneous and task-evoked brain activity negatively interact. J Neurosci. 2013;33(11):4672-82.

21. Huang Z, Zhang J, Longtin A, Dumont G, Duncan NW, Pokorny J, et al. Is there a nonadditive interaction between spontaneous and evoked activity? Phase-dependence and its relation to the temporal structure of scale-free brain activity. Cerebral Cortex. 2017;27(2):1037-59.

22. Murphy K, Fox MD. Towards a consensus regarding global signal regression for resting state functional connectivity MRI. Neuroimage. 2017;154:169-73.

23. Garrett DD, Kovacevic N, McIntosh AR, Grady CL. Blood oxygen level-dependent signal variability is more than just noise. J Neurosci. 2010;30(14):4914-21.

24. Lachaux JP, Rodriguez E, Martinerie J, Varela FJ. Measuring phase synchrony in brain signals. Hum Brain Mapp. 1999;8(4):194-208.

25. Kuramoto Y. Chemical oscillations, waves, and turbulence: Springer Science & Business Media; 2012.

26. Garrett DD, Kovacevic N, McIntosh AR, Grady CL. The importance of being variable. J Neurosci. 2011;31(12):4496-503.

27. Huang Z, Zhang J, Wu J, Qin P, Wu X, Wang Z, et al. Decoupled temporal variability and signal synchronization of spontaneous brain activity in loss of consciousness: An fMRI study in anesthesia. Neuroimage. 2016;124(Pt A):693-703.

28. Zhang J, Huang Z, Chen Y, Zhang J, Ghinda D, Nikolova Y, et al. Breakdown in the temporal and spatial organization of spontaneous brain activity during general anesthesia. Hum Brain Mapp. 2018;39(5):2035-46.

29. Cole MW, Pathak S, Schneider W. Identifying the brain's most globally connected regions. Neuroimage. 2010;49(4):3132-48.

30. Ito T, Kulkarni KR, Schultz DH, Mill RD, Chen RH, Solomyak LI, et al. Cognitive task information is transferred between brain regions via resting-state network topology. Nat Commun. 2017;8(1):1027.

31. Glasser MF, Coalson TS, Robinson EC, Hacker CD, Harwell J, Yacoub E, et al. A multi-modal parcellation of human cerebral cortex. Nature. 2016;536(7615):171-8.

32. Amunts K, Zilles K. Architectonic Mapping of the Human Brain beyond Brodmann. Neuron. 2015;88(6):1086-107.

33. Ponce-Alvarez A, Deco G, Hagmann P, Romani GL, Mantini D, Corbetta M. Resting-state temporal synchronization networks emerge from connectivity topology and heterogeneity. PLoS Comput Biol. 2015;11(2):e1004100.

34. Mitra A, Snyder AZ, Blazey T, Raichle ME. Lag threads organize the brain’s intrinsic activity. Proceedings of the National Academy of Sciences. 2015:201503960.

35. Mitra A, Snyder AZ, Hacker CD, Raichle ME. Lag structure in resting-state fMRI. J Neurophysiol. 2014;111(11):2374-91.

36. Weaver KE, Wander JD, Ko AL, Casimo K, Grabowski TJ, Ojemann JG, et al. Directional patterns of cross frequency phase and amplitude coupling within the resting state mimic patterns of fMRI functional connectivity. Neuroimage. 2016;128:238-51.

37. Deco G, Tononi G, Boly M, Kringelbach ML. Rethinking segregation and integration: contributions of whole-brain modelling. Nat Rev Neurosci. 2015;16(7):430-9.

38. Gutierrez-Barragan D, Basson MA, Panzeri S, Gozzi AJCB. Infraslow state fluctuations govern spontaneous fMRI network dynamics. 2019.

39. Wong CW, DeYoung PN, Liu TT. Differences in the resting-state fMRI global signal amplitude between the eyes open and eyes closed states are related to changes in EEG vigilance. Neuroimage. 2016;124:24-31.

40. Wong CW, Olafsson V, Tal O, Liu TT. Anti-correlated networks, global signal regression, and the effects of caffeine in resting-state functional MRI. Neuroimage. 2012;63(1):356-64.

41. Wong CW, Olafsson V, Tal O, Liu TT. The amplitude of the resting-state fMRI global signal is related to EEG vigilance measures. Neuroimage. 2013;83:983-90.

42. Chang C, Leopold DA, Schölvinck ML, Mandelkow H, Picchioni D, Liu X, et al. Tracking brain arousal fluctuations with fMRI. Proceedings of the National Academy of Sciences. 2016;113(16):4518-23.

43. Scholvinck ML, Maier A, Ye FQ, Duyn JH, Leopold DA. Neural basis of global resting-state fMRI activity. Proc Natl Acad Sci U S A. 2010;107(22):10238-43.

44. Glasser MF, Smith SM, Marcus DS, Andersson JL, Auerbach EJ, Behrens TE, et al. The Human Connectome Project's neuroimaging approach. Nat Neurosci. 2016;19(9):1175-87.

45. Van Essen DC, Smith SM, Barch DM, Behrens TE, Yacoub E, Ugurbil K, et al. The WU-Minn Human Connectome Project: an overview. Neuroimage. 2013;80:62-79.

46. Ugurbil K, Xu J, Auerbach EJ, Moeller S, Vu AT, Duarte-Carvajalino JM, et al. Pushing spatial and temporal resolution for functional and diffusion MRI in the Human Connectome Project. Neuroimage. 2013;80:80-104.

47. Barch DM, Burgess GC, Harms MP, Petersen SE, Schlaggar BL, Corbetta M, et al. Function in the human connectome: task-fMRI and individual differences in behavior. Neuroimage. 2013;80:169-89.

48. Marcus DS, Harwell J, Olsen T, Hodge M, Glasser MF, Prior F, et al. Informatics and data mining tools and strategies for the human connectome project. Front Neuroinform. 2011;5:4.

49. Glasser MF, Sotiropoulos SN, Wilson JA, Coalson TS, Fischl B, Andersson JL, et al. The minimal preprocessing pipelines for the Human Connectome Project. Neuroimage. 2013;80:105-24.

50. Daffertshofer A, Ton R, Kringelbach ML, Woolrich M, Deco G. Distinct criticality of phase and amplitude dynamics in the resting brain. Neuroimage. 2018;180(Pt B):442-7.

51. Cohen J. Statistical power analysis for the behavioral sciences 2nd edn. Erlbaum Associates, Hillsdale; 1988.